

BEHAVIOUR OF CERAMIC COMPOSITIONS ON DRYING UNDER INDUSTRIAL CONDITIONS

J.C. Jarque^(*), V. Cantavella^(*), C. Segarra^(*), G. Silva^(*),
B. Cabrera^(**), F. Gascón^(**)

^(*)Instituto de Tecnología Cerámica (ITC)
Asociación de Investigación de las Industrias Cerámicas
Universitat Jaume I. Castellón. Spain

^(**)Azteca Cerámica, S.L.

ABSTRACT

Traditionally, the drying operation has received little attention. This has partly been because dryers rarely formed the limiting stage of the production process. However, the study of the drying behaviour of ceramic bodies is of considerable interest: on the one hand because it enables establishing the time required to dry the tiles, and on the other because it provides information on the moments during drying when the tile is most sensitive.

In this study laboratory tests were carried out to determine drying kinetics, establishing how air temperature and relative humidity affect the drying process.

The evolution of tile surface moisture content was shown to differ from what might be expected on simply considering that the surface dries immediately, or that equilibrium moisture is quickly reached. The process is more complex and equilibrium between water in the liquid phase absorbed in the tiles and water vapour possibly plays a role.

The parameters that affect drying kinetics were related to the process variables (pressing pressure, pressing moisture content and bulk density), also determining other microstructural parameters such as permeability. This study enables determining, a priori, how modifying the operation conditions can affect drying.

The developed model has been applied to a vertical and a horizontal industrial dryer. The tests were conducted at Azulejera Técnica, S.A., and at Azteca Stoneware, S.L. (hereinafter Azteca).

The tile was always placed in the same position in the holder. Two J-type thermocouples were fixed to the tile top and bottom surface, connected to a data logger, monitoring tile surface temperature during the drying test. In each operation ambient air temperature and relative humidity were recorded, thus establishing air relative humidity inside the chamber. Air velocity and direction remained constant throughout the drying.

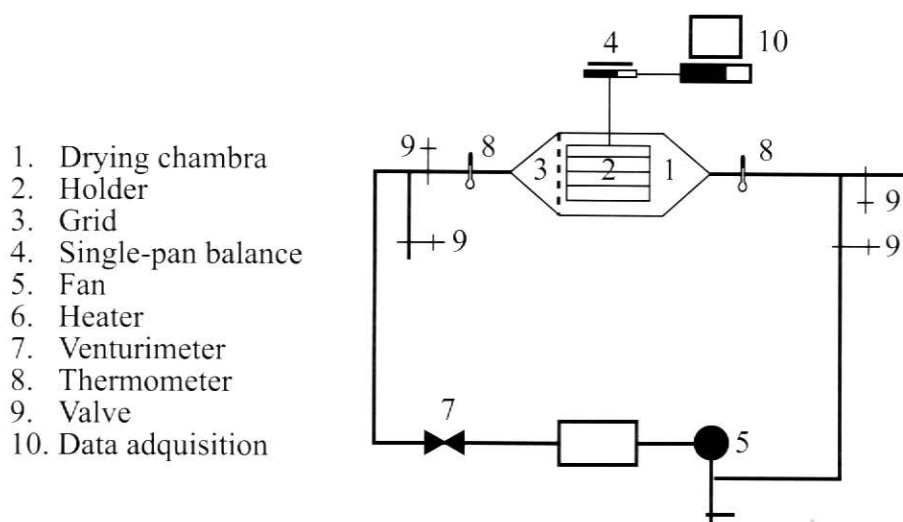


Figure 1. Scheme of the experimental drying assembly.

3.2.3 Equilibrium isotherms

The equilibrium moisture was determined (water content of a solid in equilibrium with air at a given relative humidity and temperature) for the spray-dried stoneware powder in a Heraeus Wotsch, HC 2020, climatic chamber. In this chamber the hygroscopic solid is placed in contact with air at a fixed temperature and relative humidity. When the weight of the solid remains constant, its final moisture content is measured, this being its equilibrium moisture.

The tests were carried out at three temperatures (40, 60 and 80 °C), setting three air relative humidities (25, 50 and 90%) for each temperature. These data allowed establishing the quantitative relation between the equilibrium moisture of the solid, and air temperature and relative humidity. The equilibrium isotherm of the solid was thus found at each temperature.

3.2.4 Measurement of tile surface moisture

Tile surface moisture content was measured with an appropriate near infrared sensor (calibrated for the material being studied), logging the data as a function of time. The tiles to be used in the test all had the same initial moisture content and bulk density. The experimental assembly is schematically illustrated in Figure 2.

Several experiments were carried out, varying fan rotating speed to analyse the effect of air velocity at the tile surface on drying kinetics.

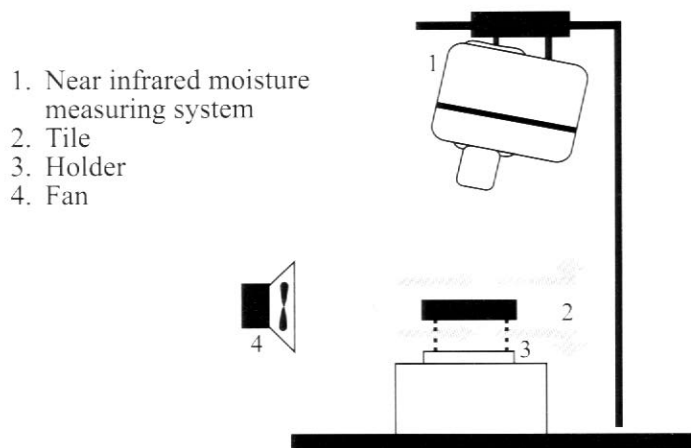


Figure 2. Scheme of the experimental assembly for measuring surface moisture (X_s).

3.2.5 Measurement of tile surface temperature and air temperature in an industrial dryer

To be able to record the temperature data (of the air and tile surface) a specially designed temperature sensing system was used. After configuring the electronic data acquisition system, it was placed in the dryer (vertical and horizontal), together with the set of sensors. This enabled establishing the tile surface and air temperature curves during the industrial drying cycle.

4. RESULTS AND DISCUSSION

4.1 ANALYSIS OF THE ISOTHERMAL MODEL

The model for drying under isothermal conditions assumes that the drying kinetics mechanism is fundamentally diffusional, making the assumption that diffusion constant D is independent of moisture content. The equation that enables determining the evolution with time of the moisture content at any point inside the tile (X) is found from^[4]:

$$\frac{\partial X}{\partial t} = D \nabla^2 X \quad [\text{Eq. 1}]$$

To solve the previous equation it is necessary to specify certain boundary conditions obeyed at the tile top and bottom surfaces (Σ), and which usually adopt the form:

$$\text{in } \Sigma: \quad T = T_x \quad [\text{Eq. 2}]$$

$$\text{in } \Sigma: \quad X = X_e \quad [\text{Eq. 3}]$$

It is also assumed that temperature is constant with time and inside the tile, and that tile surface moisture is equal to equilibrium moisture (X_e).

This equation can be integrated easily, deriving a simplified expression, valid for any value of t except for the initial moments.

$$\frac{X - X_e}{X_0 - X_e} = \frac{8}{\pi^2} \exp\left(-\frac{D\pi^2}{h^2} t\right) \quad [\text{Eq. 4}]$$

where X_0 is initial moisture and h is tile thickness.

To address the study of the isothermal model, a series of experiments was carried out on a laboratory scale, basically with a view to verifying if the conditions of the model held. To analyse the first boundary condition, temperature was measured at the tile bottom surface (T Inf) and top surface (T Sup), as well as ambient temperature inside the drying chamber where drying took place (T Amb). The results are plotted in Figure 3.

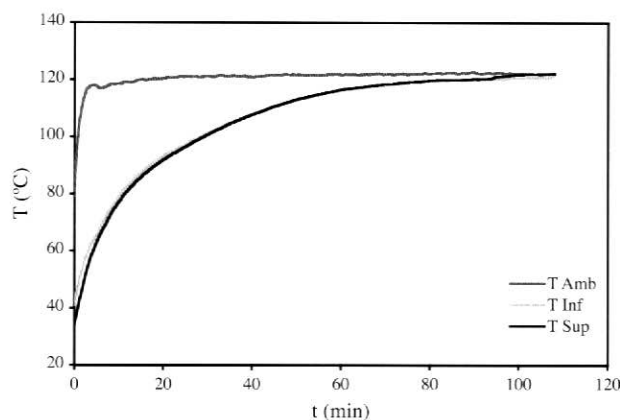


Figure 3. Comparison of chamber ambient T and tile surface T.

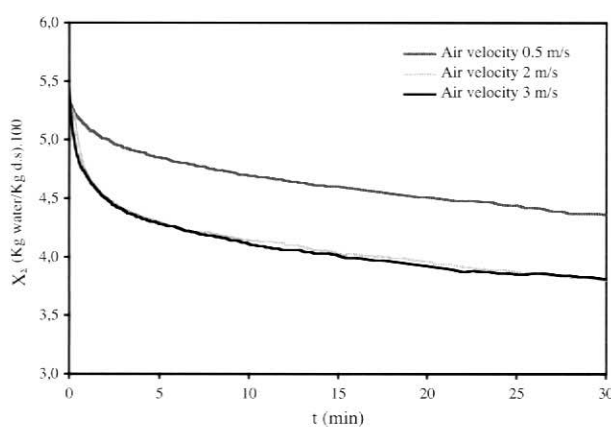


Figure 4. Variation of tile surface moisture with air velocity.

This figure shows that although the air quickly reaches the set temperature, the same does not occur with tile surface temperature. Therefore, though gas temperature is constant, drying under these conditions is not isothermal.

To verify the second boundary condition (equation 3), moisture was measured at the tile surface using the experimental assembly of Figure 2, conducting tests at different air circulation velocities (0.5, 2 and 3 m/s) for tiles with the same initial moisture content and bulk density. Ambient conditions were as follows: relative humidity 65% and temperature 25° C. The results of the test are shown in Figure 4, in which the evolution of tile surface moisture is plotted for three selected air circulation velocities. On going from 0.5 to 2 m/s a very significant change in drying rate is observed, whereas on going from 2 to 3 m/s practically no variation is found in the drying curve. This behaviour can be explained by the phases unfolding in drying. At least

two phases are involved: in the first phase, water migrates from inside the tile toward the surface by a diffusional mechanism. In the second phase, the water vapour present at the tile surface is removed by air stream drag. The increase in drying rate from 0.5 to 2 m/s is due to water vapour removal from the tile surface being favoured by convection [5]. On further raising the gas circulation velocity (step from 2 to 3 m/s), the gas velocity does not improve drying, because under these conditions, the first phase (migration of water inside the solid) is process-controlling, and is independent of gas circulation velocity.

In the three curves of Figure 4, it can be observed that tile surface moisture content does not at any moment reach equilibrium moisture, as is assumed in the second boundary condition (equation 3). This behaviour could be explained by the existence of an equilibrium between the water absorbed at the tile surface ($H_2O_{(ab)}$) and the water in a vapour state ($H_2O_{(v)}$).

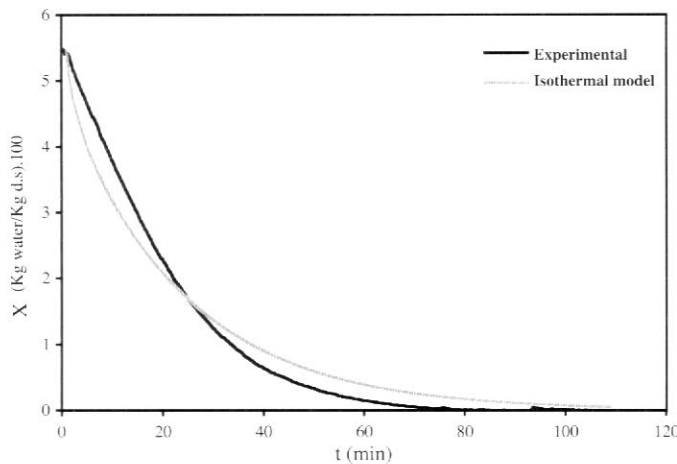
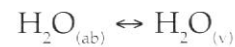


Figure 5. Fit of the isothermal model to the experimental data.

The water absorbed in the tile surface will follow a desorption process, characterised by a certain kinetics. Therefore in the drying process, when the gas circulation velocity is high, two mechanisms act: mass transfer from inside the tile to the surface by diffusion, and desorption of the water absorbed in the tile surface.

If the boundary conditions and the assumptions made are not valid, the isothermal model can be expected not to exactly fit the experimental data, as Figure 5 shows.

As a result of the foregoing, it is necessary to develop a non-isothermal model, which enables more accurately reproducing the tile drying process in industrial dryers.

4.2 DEVELOPMENT OF A NON-ISOTHERMAL MODEL

4.2.1 Mass and energy balances

The model for drying under non-isothermal conditions assumes that the moisture removal mechanism is essentially diffusional. The following equation is therefore applicable:

$$\frac{\partial X}{\partial t} = \nabla \cdot (D \nabla X) \tag{Eq. 5}$$

This expression enables establishing the variation of moisture content inside the tile with time. On the other hand, the equation of heat transmission inside the tile can be written as [6]:

$$\rho c_p \frac{\partial T}{\partial t} = k \nabla^2 T + G_E \quad [\text{Eq. 6}]$$

where:

ρ : bulk density (kg/m³)

c_p : specific heat (J/(kgK))

k : thermal conductivity (W/(mK))

The heat generation term G_E accounts for the variation of thermal energy as a result of water evaporation. If L_v is vaporisation enthalpy (at the considered temperature), heat generation can be written as:

$$\frac{G_E}{\rho} = L_v \frac{\partial X}{\partial t} \quad [\text{Eq. 7}]$$

where L_v is water vaporisation enthalpy.

Combining all the expressions yields a system of equations in partial derivatives, of the form:

$$\begin{aligned} \frac{\partial X}{\partial t} &= \nabla \cdot (D \nabla X) \\ \frac{\partial T}{\partial t} &= \nabla \cdot (\beta \nabla X) + \alpha \nabla^2 T \end{aligned} \quad [\text{Eq. 8}]$$

where β :

$$\beta = \frac{L_v D}{c_p} \quad [\text{Eq. 9}]$$

4.2.2 Dependence of diffusivity on moisture and temperature

In Eq. 8, in a first approximation, thermal conductivity (k), specific heat (c_p) and bulk density (ρ) can be considered independent of temperature and moisture. In principle, apparent diffusivity (D) can vary with temperature and moisture. However, the tests run indicate that its dependence on temperature is much more pronounced than on moisture. In fact the relation between diffusivity and temperature is usually considered given by the Arrhenius equation, i.e.:

$$D = D_0 \exp\left(-\frac{Q_D}{T}\right) \quad [\text{Eq. 10}]$$

where D_0 and Q_D are constants.

4.2.3 Boundary conditions

To solve Eq. 8 it is necessary to specify the boundary conditions. Two boundary conditions need to be kept in mind. The first affects temperature and requires experimentally determining temperature:

$$\text{in } \Sigma: T = T_\Sigma \quad [\text{Eq. 11}]$$

where Σ represents the tile boundary (surface). Obviously T_Σ will depend on time (Figure 3).

The second boundary condition defines tile surface moisture content at a given moment. It is usually assumed to be known and equal to zero, or equal to equilibrium moisture. However, as mentioned previously, this moisture content is not only not equal to equilibrium moisture, but also varies in time, even with good gas circulation conditions. For this reason, an equation is proposed that takes into account this variation in moisture with time. One of the simplest equations that obeys this requirement is:

$$\text{in } \Sigma: -\frac{dX}{dt} = k(X - X_e) \quad [\text{Eq. 12}]$$

In Eq. 12 the rate of variation in tile surface moisture content (absorbed moisture) can be taken as proportional to the difference between the moisture that exists at a given moment and the equilibrium moisture that would be reached after a sufficiently long time. This process is possibly related to a water desorption process at the tile surface. Therefore, constant k could be interpreted as the kinetic constant of the desorption process.

It is to be noted that although this equation is used to study drying, it could also be used to analyse the incorporation of moisture into the stored tiles after decoration.

The desorption constant (k) depends on temperature, also postulating an Arrhenius-type relation between k and T :

$$k = k_0 \exp\left(-\frac{\Theta_k}{T}\right) \quad [\text{Eq. 13}]$$

where k_0 and Θ_k are constants.

Finally, to be able to use Eq. 12 it is necessary to know how equilibrium moisture varies with time. Equilibrium moisture depends on air temperature and relative humidity in contact with the tile (φ); at a given temperature, the function $X_e = X_e(\varphi, T)$ is known as the "equilibrium isotherm". Although many expressions exist for $X_e = X_e(\varphi, T)$, most of which are empirical or semi-empirical, in the literature surveyed no valid equation was found for the whole range of analysed air relative humidities and temperatures. The Henderson isotherm, which is one of the most widely used in ceramic materials [7], entails the problem that the parameters on which it depends are not constant over the whole range of relative humidities, it being necessary to use two sets of parameters, one for low and another for high relative humidity.

For these reasons, a very simple empirical polynomial expression was proposed to represent the equation $X_e = X_e(\varphi)$. Keeping in mind that at $\varphi = 0$ $X_e = 0$ should hold, the polynomial of the lowest degree that allows fitting the experimental data would adopt the form:

$$X_e = c'_1\varphi + c'_2\varphi^2 + c'_3\varphi^3$$

It was empirically verified that at a given relative humidity, the variation of equilibrium moisture satisfactorily fitted an exponential equation, finally yielding the sought expression:

$$X_e(\varphi, T) = A_x e^{-\lambda T} \varphi(c_1 + c_2\varphi + \varphi^2) \quad [\text{Eq. 14}]$$

where A_x , λ , c_1 and c_2 are empirical constants.

4.3 VERIFICATION OF THE NON-ISOTHERMAL MODEL UNDER LABORATORY CONDITIONS

To be able to apply the developed model it is necessary to know the parameters that define the theoretical model (k_0 , Θ_k , D_0 and Θ_D). It is also necessary to analyse the affect of the drying cycle, tile characteristics and type of material on the parameters of the model. The system of differential equations (8) was solved using the method of implicit finite differences^[8]. The resolution algorithm was programmed in C++.

4.3.1 Study and definition of boundary conditions

Equilibrium isotherm

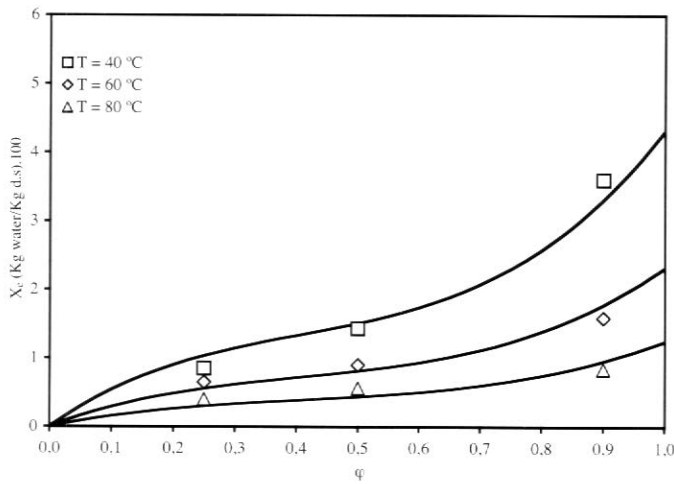


Figure 6. Fit of the equilibrium isotherm.

To be able to specify the boundary conditions (equation 12) for the stoneware material, equilibrium moisture values in different air conditions (relative humidity and temperature) are needed; for this, the procedure indicated in section 3.2.3 was followed. The values found experimentally appear in Figure 6, next to the solid line that represents the theoretical values.

The parameters of the expression that relates equilibrium moisture to air relative humidity and temperature (equation 14) for the stoneware material were as follows:

$$c_1 = 0.680 \quad A_x = 0.3291 \text{ kg agua/kg ss}$$

$$c_2 = -1.226 \quad \lambda = 0.03107 \text{ }^\circ\text{C}^{-1}$$

Desorption kinetics

Inevitably, two phases exist in the drying curves: migration of water from inside the tile to the surface and desorption at the tile surface. The former depends on thickness, while the second does not. Therefore, a way of separating both phases consists of performing drying tests with tiles that have a very small thickness, or even to work directly with a layer of spray-dried powder. This last option was chosen to determine the desorption coefficients.

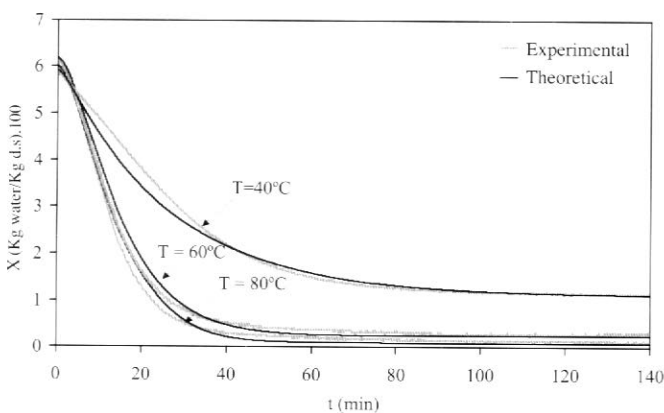


Figure 7. Fit of desorption parameters to the experimental drying curves.

To quantify the desorption coefficients, pseudo-isothermal tests (constant temperature in the drying chamber) were carried out. The material (spray-dried powder) was spread on a tray, on which a J type thermocouple was set and placed in the drying assembly holder (Figure 1) in the same position occupied by the tiles.

The material to be used for the test (stoneware) had an initial moisture content of 6%. Three drying cycles were selected with different maximum temperatures (40, 60 and 80 °C).

Using the kinetic model described in section 4.2.2, the following values were found for the desorption parameters that appear in equation 12:

$$k_0 = 100 \text{ s}^{-1} \quad \Theta_k = 3150 \text{ K}$$

The experimental results are shown in Figure 7 next to the theoretical curve, exhibiting good agreement.

4.3.2 Effect of the drying cycle

Drying cycle maximum temperature

To try and reproduce industrial drying, in which temperature does not remain constant during the whole cycle, the tile was heated from ambient temperature to maximum temperature (40, 60, 80, 100, 120, 140 °C) at a constant heating rate. The objective was to attempt to reproduce drying curves at different temperatures with a single set of parameters. If this was possible, the model would probably be applicable to an arbitrary temperature curve and, in particular, to the temperature curve of an industrial dryer.

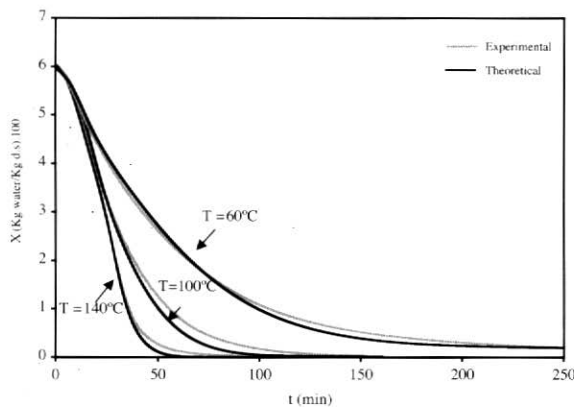


Figure 8. Effect of drying cycle maximum temperature.

The assembly employed for these tests was the one illustrated in Figure 1, in this case using tiles pressed at 6% moisture content and pressure of 250 kg/cm², holding tile thickness (8 mm) and bulk density.

Figure 8 shows the results found at three of the six test temperatures, as well as certain values determined theoretically using equation 8. The fit is observed to be very good. It should be noted that all these curves were fitted using only two diffusion parameters. The parameters found (D_0 and Θ_D) fitting the theoretical model are:

$$D_0 = 2.6 \cdot 10^{-4} \text{ m}^2/\text{s} \quad \Theta_D = 3800 \text{ K}$$

The values of k_0 and Q_k used were found in the previous section.

Tile heating rate

Up to this point, the parameters have been established that define the kinetic model for drying in all its phases for tiles pressed under the same working conditions and the applicability of the model, independently of the maximum temperature reached in the drying operation, has been verified. Another variable to be analysed is heating rate. It is very important for the kinetic model to be able to predict drying for different temperature curves, as set out in the previous section.

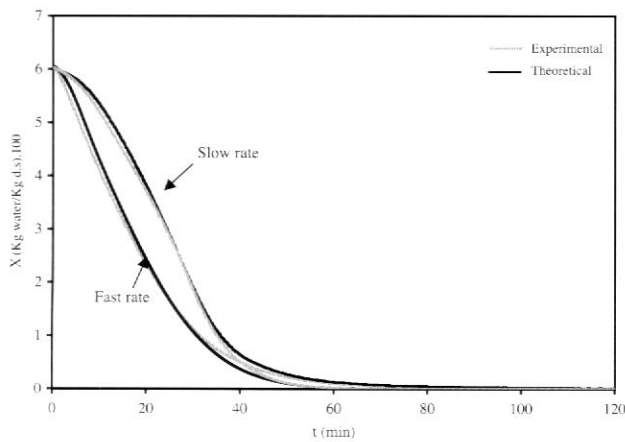


Figure 9. Effect of heating rate.

To study the role of heating rate, tiles were used formed from spray-dried powder at 6% moisture content and 250 kg/cm² pressure, holding density and thickness. The drying curve with a fast heating rate was found by placing the tile in the chamber when maximum temperature had already been reached.

Using the parameters of the kinetic model previously found for tiles pressed under the same working conditions, one can observe that the resulting theoretical curve satisfactorily fits the experimental data (Figure 9). This demonstrates that the model adapts to changes in heating rate.

4.3.3 Effect of tile characteristics on the drying operation

The previous tests focused on confirming the applicability of the kinetic model with regard to different maximum drying temperatures and changes in heating rate, but no tile-related characteristics have been varied. In practice changes can take place in tile density and thickness; it is therefore useful to know how the parameters of the drying model vary with these changes.

Effect of bulk density

First, drying tests were carried out with tiles of the same material (spray-dried powder for stoneware manufacture) pressed at different moisture contents and pressures (5, 6, 7% and 150, 250, 400 kg/cm²), which yielded a wide range of bulk densities (Table 1). Thickness was kept constant (8 mm) in all the tests, as well as the temperature curve during drying.

p(kg/cm ²)	X (%)	ρ (kg/m ³)	D ₀ (m ² /s)·10 ⁴
150	5	1943	3.6
150	7	2105	2.2
250	6	2060	2.6
400	5	2003	3.0
400	7	2150	2.0

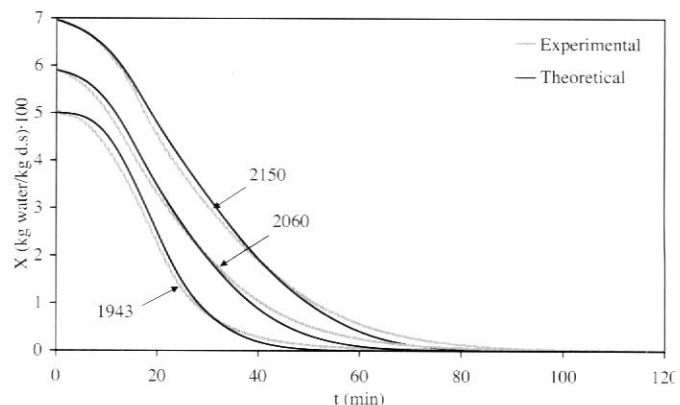


Figure 10. Effect of tile density on drying curve.

Table 1. Density and D₀ values of the test specimens used.

The parameters found are detailed in Table 1, in which D_0 one can be observed to depend on tile characteristics. The other parameters (k_0 , Θ_k and Θ_D) remain constant, their values being:

$$k_0 = 100 \text{ s}^{-1} \qquad \Theta_k = 3150 \text{ K} \qquad \Theta_D = 3800 \text{ K}$$

The fact that k_0 and Θ_k remain constant is reasonable, since they are related to the desorption process that unfolds at the tile surface, and which should therefore be independent of bulk density. The independence of Θ_D with regard to ρ was not foreseeable a priori; however it facilitates the study and interpretation of the variation of D_0 with ρ enormously.

The experimental values (drying curve), as well as the curve calculated theoretically, have been plotted in Figure 10, (to facilitate visualisation, only three of the five tests carried out are shown). Good fit can be observed.

Effect of thickness

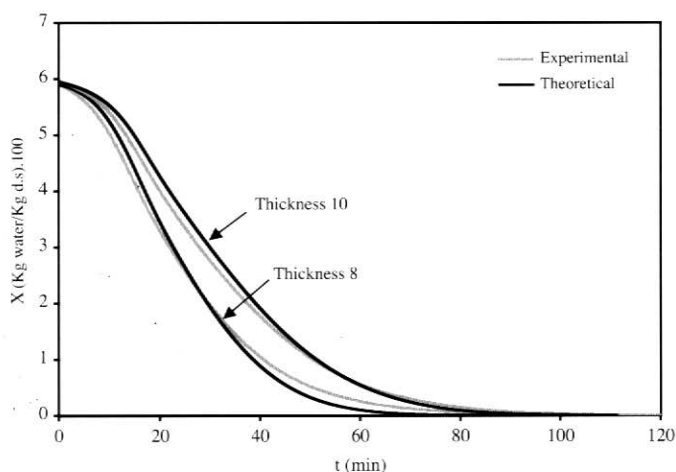


Figure 11. Effect of tile thickness on drying curve.

In these tests the effect of tile thickness on drying kinetics was analysed. The kinetic parameters used were those determined in section 4.3.2.

The test tiles were pressed at 6% moisture content and 250 kg/cm² pressure, selecting two thickness: 8 and 10 mm. The assembly used for drying was the one depicted in Figure 1, programming a drying cycle with a maximum temperature of 130 °C.

The results are plotted in Figure 11. The model is observed to fit well, confirming that the different parameters of the model are intrinsic to the material, and do not depend on tile geometry.

4.3.4 Effect of type of material and drying kinetics

With a view to extending the study to other types of materials, drying tests were conducted with test specimens made from spray-dried powder with a “porosa” composition. Obviously in this case, parameters k_0 , Θ_k , D_0 and Θ_D could be different, since the nature of the material is different.

The tiles used in the test were pressed at a moisture content of 6% and pressure of 250 kg/cm², keeping thickness steady at 8 mm. Two drying cycles were conducted, varying the heating rate. The parameters that yielded the best fit were:

$$k_0 = 200 \text{ s}^{-1} \qquad D_0 = 3.3 \cdot 10^{-4} \text{ m}^2/\text{s}$$

$$\Theta_k = 3000 \text{ K} \qquad \Theta_D = 3800 \text{ K}$$

Figure 12 depicts the experimental data and theoretical results, confirming good agreement.

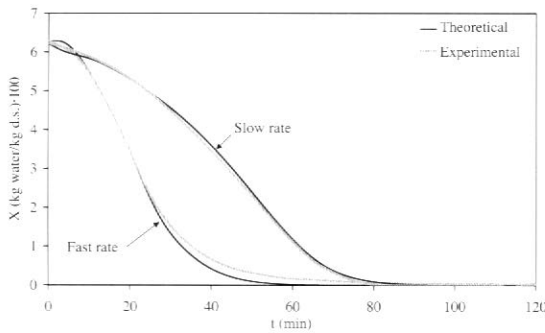


Figure 12. Effect of the drying cycle on "porosa" tiles.

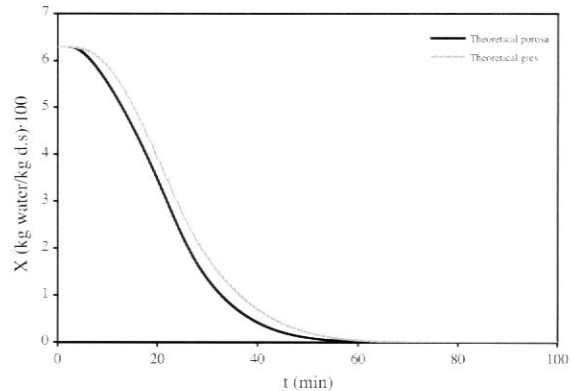


Figure 13. Comparison between theoretical stoneware and "porosa" tile curves.

Direct comparison of the parameters found for stoneware and porosa tile bodies is difficult, since four parameters are involved and the drying curves depend on all of these. It is therefore more useful to theoretically calculate the drying curve that would be found for tiles made with the two materials, at constant tile thickness and bulk density. Figure 13 presents the result of this calculation. It shows that the porosa composition dries just a little faster than the stoneware composition, though the differences are not very significant. This contrasts with the fact that in industry, stoneware tiles typically are more difficult to dry. The reason for this is that stoneware tiles usually have lower porosity (greater bulk density) and are thicker, so that industrially, the biggest differences between stoneware and porosa tile drying does not stem from the body composition but from different forming conditions.

4.4 RELATION BETWEEN MICROSTRUCTURE AND DRYING KINETICS

The drying kinetics defined in section 4.2. consists of two phases: the water migration phase from inside the tile to the tile surface (controlled by diffusivity) and the phase in which water held in the tile surface transfers to the gas phase (desorption). This section will analyse the effect of tile microstructure (characterising it by bulk density and the permeability coefficient) on the parameters that define both phases.

4.4.1 Relation between tile microstructure and diffusion kinetics

Coefficient D_0 (Table 1) only depends on ρ ; i.e., at a given density value it is independent of moisture content and pressing pressure. Figure 14 plots $\log D_0$ versus the logarithm of density, showing that the relation is linear, that is:

$$\ln D_0 = a_D + b_D \ln \rho$$

On the other hand the permeability coefficient (obtained experimentally for tiles with the same characteristics) also depends only on bulk density, the relation between both (Figure 14) being:

$$\ln K_p = a_K + b_K \ln \rho$$

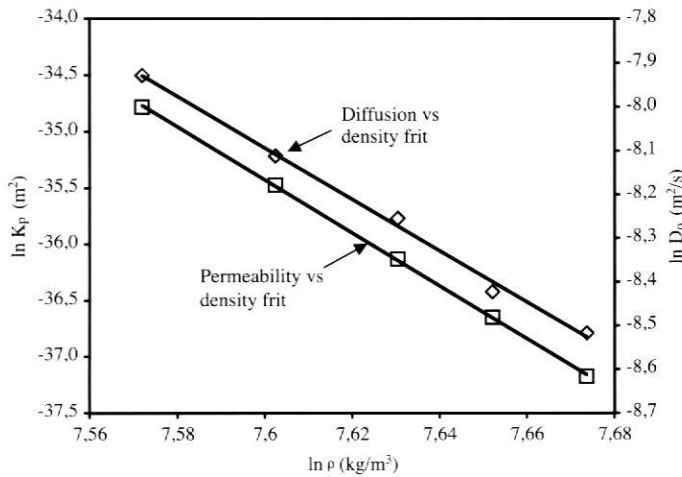


Figure 14. Plot of D_0 and K_p with density.

All this enables establishing a direct relation between the diffusion coefficient and tile microstructure (characterised by the permeability coefficient).

The two foregoing expressions allow deriving an interesting equation that relates a characteristic drying parameter D_0 to a property (K_p) that quantifies the resistance of a porous material to gas flow through the material:

$$D_0 = aK_p^b \quad [\text{Eq. 15}]$$

When D_0 is expressed in m^2/s and K_p in m^2 constants a and b adopt the values:

$$a = 0.57 \quad b = 0.25$$

4.4.2 Relation between tile microstructure and desorption kinetics

Desorption kinetics only depends on the type of material and particle size distribution (specific surface area) and not on material bulk density. The experimental results found corroborate these facts, because using the same desorption parameters enables fitting the kinetic model to tiles with different densities (Figure 10).

4.5 APPLICATION OF THE KINETIC MODEL TO INDUSTRIAL DRYING

To verify the industrial applicability of the kinetic model to the drying curve simulation, industrial tests were conducted at Azteca in a vertical and a horizontal dryer. It is necessary to keep in mind that the ultimate objective of this study was to better understand and optimise drying under industrial conditions, hence the relevance of these tests.

To define the boundary conditions, it is necessary to know tile surface temperature, for which a temperature sensing system was used. Unfortunately, the boundary conditions require knowing the temperature bounding the whole tile and the temperature sensor only determines the temperature at the tile top surface and of the air in contact with the tile. To be able to carry out the calculations it was assumed that the tile bottom surface temperature was the same as that of the top.

Parameters k_{0r} , Θ_k , D_{0r} and Θ_D used in the simulation were those found experimentally for the stoneware composition. Tiles were collected at the dryer exit to compare the experimental moisture content with the theoretically calculated value.

4.5.1. Application of the model to a vertical dryer

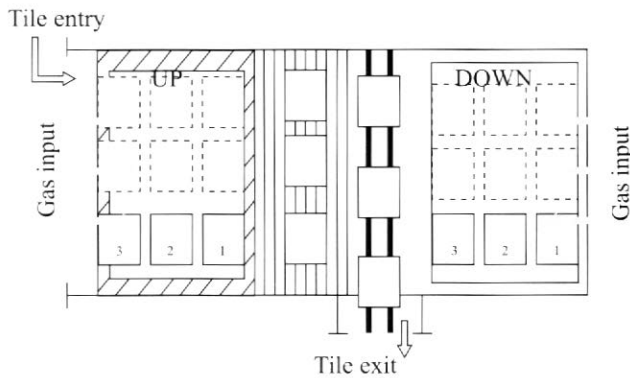


Figure 15. Arrangement of the three sensors in the tile deck in the dryer.

The first industrial test was carried out in a vertical dryer at the Azteca plant. During the test, stoneware measuring 41x41 cm was being dried. In this dryer, nine tiles go into a deck. Three positions were selected to set the measuring sensors (positions indicated in Figure 15).

Figure 16 shows the evolution of gas temperature inside the dryer versus its position. It can be observed that after the gases enter the dryer, an abrupt rise in temperature takes place, being more pronounced in position 3. This is because the hot gases that are fed into the dryer first come into contact with the sensors located in position 3.

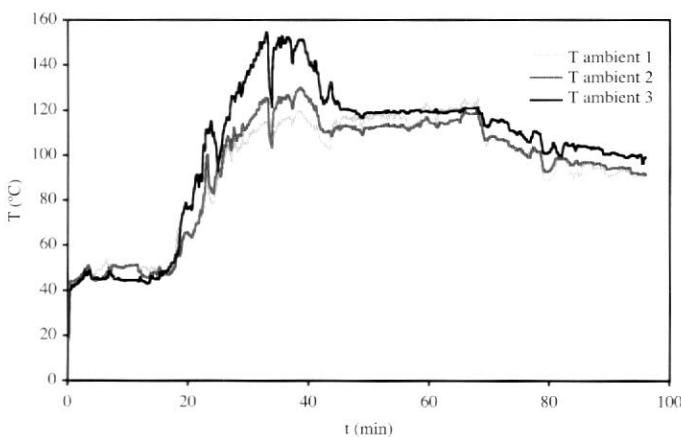


Figure 16. Gas temperature distribution in the dryer .

At 40 minutes, temperatures descend on entering the area where the baskets change their direction. The drop in temperature is due to two factors: to the low gas circulation velocity and the fact that gases are not used directly from the burners (gases extracted from the up zone). Temperatures stabilise on entering the down zone (effect of the second burner) at 50 minutes, because in this zone the temperature is lower. A slight inversion of the temperatures is noticed because now the sensor in position 1 is the one receiving the incoming gas. Slightly before minute 80, a stabilisation zone is encountered.

To carry out the simulation of the vertical dryer, the tile surface temperature curve was used (Figure 17), together with the following values:

Tile mean starting moisture content: 5.61% (kg water/kg dry solid)
 Mean tile thickness (without rib): 9.7 mm.
 Dry bulk density: 2055 (kg/m³)

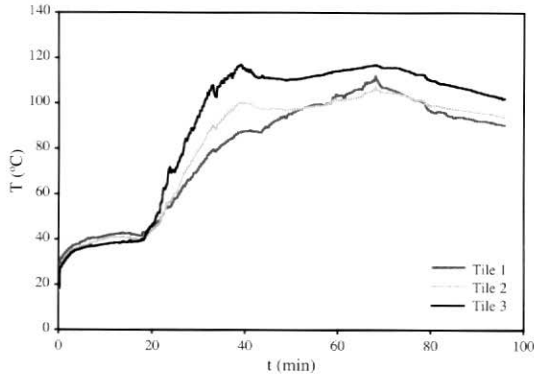


Figure 17. Temperature distribution at the tile surface in the dryer.

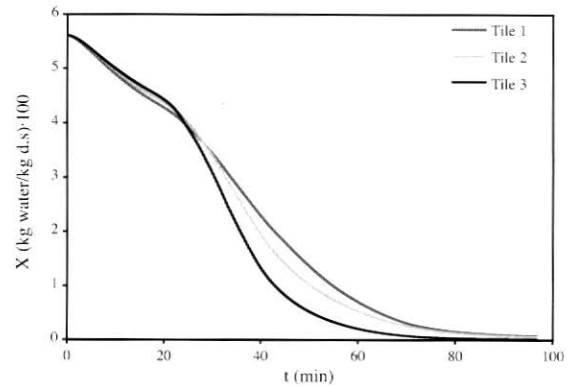


Figure 18. Tile drying curve in the dryer.

The theoretical curves of moisture content evolution simulated with the kinetic model are depicted in Figure 18. They show that after 20 minutes, drying rate rises (curve slope), this being more pronounced in tile 3, because it receives the gas input more directly. This increase in the drying rate is related to the rise in temperature that the tiles undergo at this point.

	X (%)	
	exper.	theor.
Tile 1	0.18	0.16
Tile 2	0.16	0.14
Tile 3	0.15	0.10

Table 2. Comparison of theoretical and experimental moisture content at the dryer exit.

The final moisture content values found with the theoretical model are given next to those obtained experimentally in Table 2, demonstrating good agreement and thus confirming the industrial applicability of the developed model.

4.5.2 Application of the model in a horizontal dryer

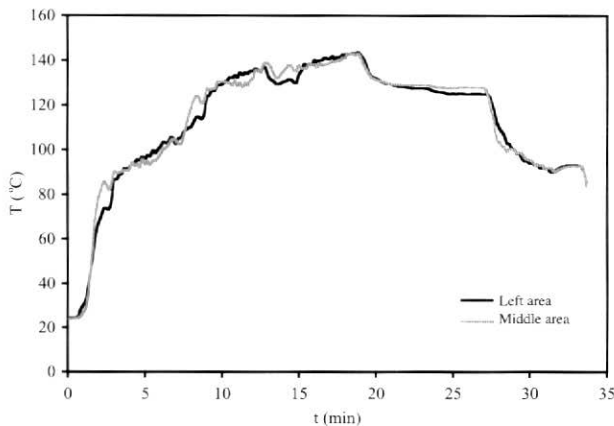


Figure 19. Gas temperature distribution inside the dryer.

The second industrial test was carried out in a horizontal dryer, at the Azteca plant. During testing stoneware tiles measuring 31x31cm were being dried. In this dryer eight tiles go into a deck, and there are five decks.

Four temperature sensors were placed in the centre deck, two on the left side and two in the middle, registering gas and tile surface temperature. This allowed monitoring possible traverse temperature gradients inside the dryer.

Analysis of the graph comparing the gas temperature curves in the dryer (Figure 19) shows that the difference is not significant, unlike what occurred in the vertical dryer. For this, the drying curve was only calculated in one position, using the tile surface temperature curve shown in Figure 20. The data used in the calculation relating to the tiles were as follows:

Tile mean starting moisture content:	5.81% (kg water/kg dry solid)
Mean tile thickness (without rib):	7.6 mm.
Dry bulk density:	2055 (kg/m ³)

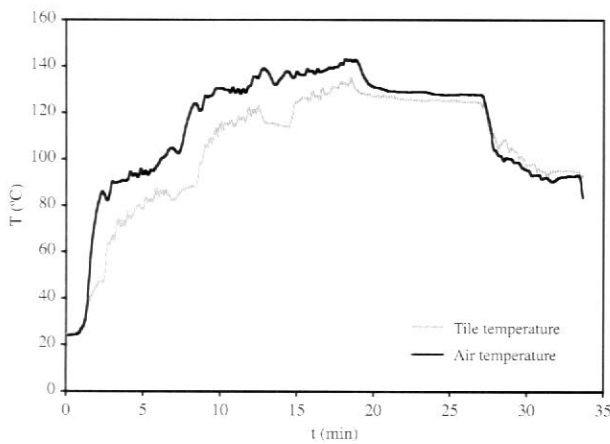


Figure 20. Comparison of gas and tile surface temperature.

The simulation of the drying curve is shown in Figure 21, in which it can be observed that the value of the moisture content reached theoretically is very similar to the one reached experimentally. In this drying curve it is more difficult to appreciate the changes in drying rate (Φ), so that this rate has been plotted together with the temperature curve throughout the drying cycle (Figure 22). The correlation can be observed between the temperature increase peaks and those of drying rate increase. After minute 20 the drying rate decreases noticeably, although temperature does not. This is because, after minute 20 the moisture content has

already largely decreased, and the diffusional phase is slower as the moisture content gradients inside the tile are smaller.

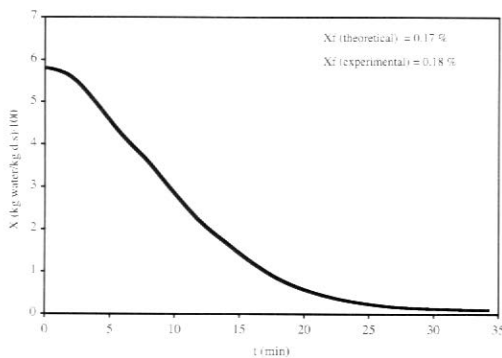


Figure 21. Tile drying curve in the dryer.

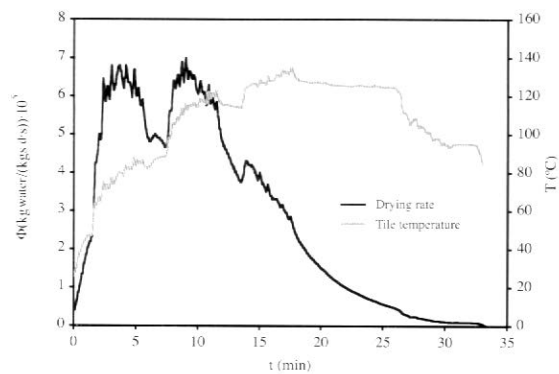


Figure 22. Gas temperature and drying rate.

5. CONCLUSIONS

- The evolution of tile surface moisture content during drying has been analysed. It was observed that this moisture does not reach an equilibrium value quickly. A desorption mechanism has been postulated to explain this behaviour.

- A model is proposed that takes into account a diffusion phase together with a desorption phase, both under non-isothermal conditions, which enables explaining the drying curves found in the laboratory under various drying rate and maximum temperature conditions.
- The effect of modifying forming conditions (moisture content and pressing pressure) on the parameters of the model was studied. It was concluded that of the four parameters involved in the model, only one (D_0) depends on the forming variables, being a function of density and not separately of moisture content and pressing pressure.
- A relation has been established between D_0 and tile permeability (K_p). This relation is especially interesting because it establishes a connection between the ease of drying and the resistance that a porous tile offers to gas flow.
- Temperature measurements were carried out in gases and at the tile surface, inside a horizontal and a vertical dryer, establishing that the vertical dryer presents greater heterogeneities in temperature than the horizontal dryer.
- Finally, the model was applied to the two studied industrial dryers (horizontal and vertical). It was shown that the model enables reproducing tile residual moisture content very well at the dryer exit.

6. REFERENCES

- [1] ESCARDINO, A.; GALLEGU, M.A.; FELÍU, C.; BARBA, A. and SÁNCHEZ, E. Drying of Ceramic Materials Shaped by Unidirectional Pressing: I Kinetic Model. *Br. Ceram. Trans.*, 92 (5), 197-202, 1993.
- [2] ESCARDINO, A.; JARQUE, J.C.; MORENO, A. and DE LA TORRE, J. Secado de Materiales Cerámicos (II). Cinética del secado de piezas cerámicas de pavimento y revestimiento. *Modelos dinámicos. Técnica Cerámica*, 190, 34-42, 1991.
- [3] MALLOL, G.; CANTAVELLA, V.; FELIU, C. and LLORENS, D. Study of ceramic tile drying under non-isothermal conditions and its industrial application. IN: Euroceramics VII: Part 3. Sessions M3, M4, M6, M7. M8, miscellaneous. Uetikon-Zurich: Trans Tech Publications, [2001]. pp. 1755-1758.
- [4] MUJUMDAR, A.S. (Ed.). *Advances in Drying*. Montreal: McGill University, 1980.
- [5] BARBA, A.; ESCARDINO, A.; MORENO, A. y NEGRE, F. Secado de soportes cerámicos para pavimento de monococción. XXX Congreso Nacional de Cerámica y Vidrio. Santiago de Compostela, 30 September - 4 October, 1990.
- [6] INCROPERA, F.P. and DE WITT, D.P. *Fundamentals of Heat and Mass Transfer*. 3rd ed. New York: John Wiley & Sons, 1990.
- [7] ESCARDINO, A.; JARQUE, J.C.; MORENO, A. y DE LA TORRE, J. Secado de materiales cerámicos (I) Consideraciones generales. *Isotermas de equilibrio. Técnica Cerámica*, 185, 452-462, 1990.
- [8] CELIA, M.A. and GRAY, W.G. *Numerical Methods For Differential Equations: Fundamental Concepts For Scientific & Engineering Applications*. Englewood Cliffs [New Jersey]: Prentice-Hall, 1991.